

Quarkyonic matter pieces together the hyperon puzzle

Yuki Fujimoto,^{1,2,3,*} Toru Kojo,^{4,5,†} and Larry McLerran^{1,‡}

¹*Institute for Nuclear Theory, University of Washington, Box 351550, Seattle, WA 98195, USA*

²*Interdisciplinary Theoretical and Mathematical Sciences Program (iTHEMS), RIKEN, Wako 351-0198, Japan*

³*Department of Physics, University of California, Berkeley, CA 94720, USA*

⁴*Theory Center, IPNS, High Energy Accelerator Research Organization (KEK), 1-1 Oho, Tsukuba, Ibaraki 305-0801, Japan*

⁵*Department of Physics, Tohoku University, Sendai 980-8578, Japan*

(Dated: October 31, 2024)

Matter composed of hyperons has been hypothesized to occur in neutron stars at densities slightly above the nuclear saturation density and in many descriptions gives rise to a significant softening in the equation of state (EoS). This softening would be at odds with the constraints from neutron star observations and ab initio nuclear matter computations at low density. This inconsistency is known as the hyperon puzzle. We show that Quarkyonic Matter models, which take into account the quark substructure of baryons, can mitigate the hyperon puzzle. We demonstrate two important consequences of the quark substructure effects. First, the hyperon threshold is shifted to a higher density as neutrons preoccupy the phase space for down quarks, preventing the emergence of hyperons at low energy. Secondly, the softening in the EoS becomes mild even above the hyperon threshold density because only little phase space is available for low-energy hyperons; increasing hyperon density quickly drives hyperons into the relativistic regime. In this work, we illustrate these two effects for a matter composed of charge-neutral baryons, using the ideal dual Quarkyonic (IdylliQ) model for three flavors. This model incorporates the Quarkyonic duality and allows us to manifestly express the quark Pauli blocking constraints in terms of the baryon occupation probability. The extension to neutron star matter is also briefly discussed.

I. INTRODUCTION AND SUMMARY

A. Motivation and background

Identifying the inner core composition of neutron stars is an important challenge in modern nuclear physics. Currently, there is no consensus on the core composition due to the lack of a reliable calculation of the equation of state (EoS) at baryon densities above $n_B \gtrsim 2n_{\text{sat}}$, where $n_{\text{sat}} \simeq 0.16 \text{ fm}^{-3}$ is the nuclear saturation density (see, e.g., [1] and references therein for the recent development at $n_B \lesssim 2n_{\text{sat}}$).

At densities higher than $2n_{\text{sat}}$, hyperons are expected to appear (see, e.g., Refs. [2, 3] for reviews). Once the neutron chemical potential μ_n exceeds the threshold, neutrons on the Fermi surface undergo weak decays into hyperons Y , which forms a new Fermi sea with chemical potential $\mu_Y = \mu_n$. In a typical hadronic EoS, the onset of hyperons is around $n_B \simeq 2\text{--}3 n_{\text{sat}}$. Unless there is strong repulsion between nucleons N and hyperons, a stiffer nuclear EoS lowers the onset of hyperons because μ_n at a given n_B is larger as the EoS becomes stiffer, so μ_n can reach the hyperon thresholds at lower n_B [4]. In fact, stiffening of the EoS at a relatively low density, around $1.5 n_{\text{sat}}$, is established phenomenologically [5]. Also, recent lattice-QCD suggests that the N - Y interaction is weaker than N - N interactions [6, 7]. For example, the hyperon single-particle potentials $U_Y(k)$ in nuclear matter from the lattice-QCD data are $U_\Lambda(0) \simeq -28 \text{ MeV}$ and $U_\Sigma(0) \simeq 15 \text{ MeV}$ [7]. The value of U_Λ is also consistent with the empirical value inferred from Λ -hypernuclei data [8]. This implies that N - Λ and N - Σ interaction on average are weakly attractive and repulsive, respectively, but their effects on the hyperons thresholds are almost negligible. The YNN three-body interactions have also been studied by confronting theoretical calculations with Λ -hypernuclei by varying atomic numbers [8–10].

It has been known that the appearance of hyperons reduces the maximum mass of neutron stars [11–13]. Such reduction is problematic as a small maximum mass is in tension with the current precise mass measurement of heavy neutron stars [14–16], and this problem is known as the *Hyperon Puzzle*. This problem is caused by the softening of the EoS, i.e., the pressure becomes small at a given energy density. There are two important effects responsible for such softening. Firstly, since hyperons are nonrelativistic right above their thresholds, their inclusion scarcely increases the pressure while the energy density increases. Also, since there are a plethora of hyperon species, the EoS

* yfujimoto@berkeley.edu

† torukojo@post.kek.jp

‡ mclerran@me.com

becomes softer at the thresholds for every species of hyperon. There are several possible resolutions to the hyperon puzzle. The hyperon puzzle might be resolved by adding additional repulsion in the interaction involving hyperons, e.g., the in-medium modifications of hyperon potentials [17, 18], or adding three-body interactions [19].

Among several possible resolutions to the hyperon puzzle, one direction is to assume the existence of quark matter inside neutron stars realized either by a phase transition at sufficiently low density [20–23] or by a continuous crossover [24–30]. These studies suggest that treating the strangeness in terms of quarks may mitigate the hyperon problems. However, the realization of quark matter at high density may not be as simple as conventionally considered [31]. Indeed, weak-coupling QCD at a large number of colors N_c implies the possible picture of quarks remaining confined even though the bulk thermodynamic properties are described in terms of the quark degrees of freedom [32]. This is known as the concept of Quarkyonic Matter.

Quarkyonic matter is a matter composed of the quark Fermi sea with the baryonic Fermi surface [32–36]. Quarks near the Fermi surface are trapped into baryons until the color screening caused by quarks cuts off confining gluons. With this consideration the range of the quark chemical potential μ for Quarkyonic matter descriptions is estimated to be $\Lambda_{\text{QCD}} \lesssim \mu \lesssim \sqrt{N_c} \Lambda_{\text{QCD}}$ [32].

In this paper, we propose a solution to the hyperon puzzle based on Quarkyonic Matter. Our solution is illustrated in the recently proposed ideal gas model of Quarkyonic matter, IdylliQ model, which allows us dual descriptions for the occupation densities of quarks and baryons from nuclear to quark matter [37]. In purely baryonic language, the surprising feature is the formation of the momentum shell structure; the constraints from the quark Pauli principle lead to strong suppression of the baryon occupation densities at low momenta while baryons at higher momenta are free of such constraint. The emerging picture is a momentum space shell structure of baryons at the surface of a Fermi sea with the Fermi sea filled by quarks [32, 38, 39] as originally conjectured in Ref. [32]. This description has been applied in the context of neutron-star phenomenology [38] and also in nuclear matter properties [40, 41].

Our treatment of isospin and strangeness content of nuclear matter is based on the IdylliQ model which has the advantage over the previous work on Quarkyonic matter models based on specific forms of baryon occupation densities [42–45]. In the IdylliQ model, we manifestly determine baryon occupation densities by keeping track of the occupation densities of all quark species and examining the quark Pauli blocking effects on each baryon. These features allow us to derive the evolution of the quark distribution which smoothly connects the flavor asymmetric baryonic matter to flavor asymmetric quark matter. Such evolution is described by extrapolating the phenomenological parametrization based on the flavor symmetric matter. In this work, we spell out how to construct Quarkyonic matter in the presence of large isospin asymmetry and/or strangeness. To present main ideas within analytic forms, in this work, we focus on a system made of charge-neutral baryons with spin 1/2, $n(udd, I = 1/2)$, $\Lambda^0(uds, I = 0)$, $\Sigma^0(uds, I = 1)$, and $\Xi^0(uds, I = 1/2)$. Including charged particles such as protons and electrons requires numerical calculations and will be presented in the forthcoming paper.

B. Summary of the results

The hyperon puzzle will be solved within Quarkyonic Matter by considering the quark substructure of baryons. This Quarkyonic solution arises because, in neutron matter, one cannot insert a strangeness $S = -1$ and charge neutral $Q = 0$ baryon without that baryon having a down quark in it, but in Quarkyonic Matter, the down quark Fermi sea is filled. The first available baryon state with strangeness which is electrically neutral and has no down quark in it is the Ξ^0 baryon composed of two strange quarks and an up quark. It is the purpose of this paper to demonstrate this and explore the consequences for the EoS.

In the following, for simplicity, we will ignore small isospin splitting in the mass, e.g., $M_{\Lambda^0} = M_{\Sigma^0}$. The main results of this paper are two-fold:

1. The threshold of the $S = -1$ hyperons is shifted from $\mu_B = M_Y$ to $2M_Y - M_N$, where M_Y and M_N are the mass of hyperons with strangeness $S = -1$ and nucleons, respectively. The shifted threshold $2M_Y - M_N$ for $S = -1$ hyperons turns out to be very close to the threshold of the charge-neutral $S = -2$ hyperon Ξ^0 , which is not affected by the down quark states and remains at M_{Ξ^0} .
2. The EoS is softened mildly by $S = -1$ hyperons, but not as strongly as would be the case if the quark substructure of baryons was not properly accounted for. The bulk of the softening in the EoS comes from the Ξ^0 hyperon.

Both these points make the hyperon contribution to the EoS less important and thus works toward the resolution of the hyperon puzzle. Hyperons at low momenta appear in the system with a low probability and thus affect the EoS only weakly. In this regard, a large number of hyperon species is no longer crucial because hyperons that have a d -quark in them suppress one another to occupy the limited phase space for d -quarks. Meanwhile, hyperons at high

momenta are almost free from the pre-occupied phase space, but those hyperons at high momenta not only increase energy density but also the pressure significantly, and hence do not soften the EoS much. Once the Ξ^0 appears, there is a significant softening in the EoS. Nevertheless, the shifted threshold is high enough so that it may not greatly affect the maximum mass of neutron stars.

In this work, after reviewing the IdylliQ model for a flavor symmetric setup in Sec. II, we first consider the inclusion of $S = -1$ hyperons only as the low-lying $S = -1$ hyperons are usually the main cause of the hyperon puzzle. Section III is mainly devoted to such analysis with $S = -1$. However, as we discussed above, the shifted threshold for $S = -1$ hyperons turns out to be very close to that of Ξ^0 . Therefore, we also need to take into account Ξ^0 at the threshold of the $S = -1$ hyperons. We will defer such analysis to the discussion section IV. We explicitly incorporate Ξ^0 and discuss its impact in Sec. IV A.

II. PRELIMINARIES: FLAVORLESS IDEAL DUAL QUARKYONIC (IDYLLIQ) MODEL

In this section, we review the details of the ideal dual Quarkyonic (IdylliQ) model, which is necessary to understand the content of the current paper. This is an elaboration of the work presented in Ref. [37], with some extra detail included. The results of this section will be needed for our later analysis.

A. Model

We assume a duality relation between the momentum distribution function for quarks with a given color $f_q(q)$ and the baryon distribution $f_B(k)$ as (we denote: $\int_k \equiv \int \frac{d^d \mathbf{k}}{(2\pi)^d}$ with $d = 3$) [46, 47].

$$f_q(q) = \int_k \varphi(\mathbf{q} - \frac{\mathbf{k}}{N_c}) f_B(k). \quad (1)$$

Here φ represents a single quark momentum distribution in a single baryon state. As quarks are confined in a spatial domain of the baryon size $\sim \Lambda_{\text{QCD}}^{-1}$, $\varphi(q)$ is spread to momenta of $\sim \Lambda_{\text{QCD}}$. Adding the quark contributions from each baryon leads to quark distributions in dense matter. Here, for symmetric nuclear matter, we include a spin-isospin degeneracy factor $g = 4$. For pure neutron matter, the factor is $g = 2$. The extension for multi-flavors and multi-baryon species will be discussed in the next section.

The normalization is $\int_q \varphi(q) = 1$. The dual expression of the baryon number that follows from Eq. (1) is

$$n_B = g \int_k f_B(k) = g \int_q f_q(q). \quad (2)$$

Here f_q is defined for a fixed color, $f_q \equiv f_q^R = f_q^G = f_q^B$ with which $n_B = n_q^R = n_q^G = n_q^B$.

For a Hamiltonian or energy density, we neglect all interactions other than that tacitly included to confine quarks into a baryon. The energy densities are simply

$$\varepsilon_B[f_B] = g \int_k E_B(k) f_B(k). \quad (3)$$

The energy of a baryon is $E_B(k) = \sqrt{M_B^2 + k^2}$. If we assume a simple additive quark model, one can write the baryon energy as

$$E_B(k) = N_c \int_q E_q(q) \varphi(\mathbf{q} - \mathbf{k}/N_c), \quad (4)$$

where E_q is defined through this relation. The following relation readily follows

$$\varepsilon_B[f_B] = g \int_q E_q(q) [N_c f_q(q)] = \varepsilon_q[f_q]. \quad (5)$$

This is the duality for the energy density. The expression with f_q is more useful when we examine EoS from the quark matter viewpoint.

In this work, we keep using the same φ from low and high densities. In reality, φ can be modified by quark exchanges as well as structural changes in baryons. All these effects will be considered elsewhere.

In order to determine the optimized distributions for baryons and quarks, we minimize the energy density functional with a given n_B by varying f_B (or f_q) at each momentum. It is tempting to introduce the Lagrange multiplier to impose the fixed n_B constraint, but the current problem with infinitely many variables (f_B at each k) does not satisfy the conditions requested for the Lagrange multiplier method which demands the existence of the multiplier λ such that $\delta\varepsilon/\delta f_B(\mathbf{k}) = \lambda\delta n_B/\delta f_B(\mathbf{k})$ for all \mathbf{k} . Hence we use the canonical method in which we manifestly fix n_B . The constraint is

$$0 = \int_k \delta f_B(k). \quad (6)$$

A variation which satisfies the constraint is

$$\delta f_B(\mathbf{k}_1) + \delta f_B(\mathbf{k}_2) = 0, \quad (7)$$

which simply means we move a particle from \mathbf{k}_2 to \mathbf{k}_1 . The change of energy associated with such change is

$$\delta\varepsilon_B = E_B(\mathbf{k}_1)\delta f_B(\mathbf{k}_1) + E_B(\mathbf{k}_2)\delta f_B(\mathbf{k}_2) = [E_B(\mathbf{k}_1) - E_B(\mathbf{k}_2)]\delta f_B(\mathbf{k}_1). \quad (8)$$

If $E_B(\mathbf{k}_1) < E_B(\mathbf{k}_2)$, the energy is reduced by increasing $f_B(\mathbf{k}_1)$ and reducing $f_B(\mathbf{k}_2)$ at the same amount. In particular, if we set $|\mathbf{k}_2|$ to k_{sh} which is the largest possible momentum for nonzero f_B , then a positive $\delta f_B(\mathbf{k})$ with $|\mathbf{k}| \leq k_{\text{sh}}$ always reduces the energy. This describes a process in which a particle with the momentum \mathbf{k}_{sh} decays into a particle with \mathbf{k} .

With $|\mathbf{k}_2| = k_{\text{sh}}$, the number-conserving variation of the energy is defined to be

$$g^{-1} \frac{\delta' \varepsilon_B}{\delta' f_B(\mathbf{k})} \equiv g^{-1} \left(\frac{\delta\varepsilon_B}{\delta f_B(\mathbf{k})} - \frac{\delta\varepsilon_B}{\delta f_B(\mathbf{k}_{\text{sh}})} \right) = E_B(k) - E_B(k_{\text{sh}}). \quad (9)$$

The slope is positive for $k \geq k_{\text{sh}}$, so $f_B(k) = 0$ is favored. For $k \leq k_{\text{sh}}$, larger values of $f_B(k)$ are favored, but whether $f_B(k)$ reaches 1 (the maximum) or not depends on the quark Pauli blocking constraint. But expressing the constraint in terms of f_B is a nontrivial problem and this is the major difficulty to solve the minimization problem with the constraint. In the IdylliQ model, we choose a specific form of φ that allows us to invert the sum rule and express f_B in terms of f_q . Then the minimization problem with the constraint can be solved explicitly.

B. A solvable model and its solution for the phase-space distributions

In the IdylliQ model, we choose the following distribution for φ ,

$$\varphi(\mathbf{q}) = \frac{2\pi^2}{\Lambda^3} \frac{e^{-q/\Lambda}}{q/\Lambda}, \quad (10)$$

which is the inverse of a linear differential operator $\hat{L} = -\nabla_q^2 + \frac{1}{\Lambda^2}$ where Λ is some scale parameter characterizing the size of baryons. Applying this operator to Eq. (1), we find a local relation between f_B and f_q ($d = 3$),

$$f_B(N_c q) = \frac{\Lambda^2}{N_c^d} \hat{L}[f_q(q)]. \quad (11)$$

The candidates of local solutions for f_q are the boundary values $f_q = 1$ and those dual to $f_B = 0$ and 1. The f_q dual to $f_B = 0$ and 1 are determined as follows. The most general solution for $f_B = 0$ is

$$f_q^{f_B=0}(q) = c_+ y_+(q) + c_- y_-(q), \quad (12)$$

where $y_{\pm}(q) = e^{\pm q/\Lambda}/q$ satisfying $\hat{L}[y_{\pm}] = 0$. Meanwhile $f_B(N_c q) = 1$ can be obtained as

$$f_q^{f_B=1}(q) = N_c^d + d_+ y_+(q) + d_- y_-(q). \quad (13)$$

The range of constants c_{\pm} and d_{\pm} are constrained by the condition $0 \leq f_q(q) \leq 1$.

We now put the candidates of solutions together. Before quark states are saturated, however, we do not have to consider the quark Pauli blocking constraint and one can readily determine the baryon distribution as

$$f_B(k) = \Theta(k_{\text{sh}} - k), \quad (14)$$

and we can substitute it into the sum rule. The solution for $f_q(q)$ takes the form

$$f_q(q) = f_q^{f_B=1}(q)\Theta(q_{\text{sh}} - q) + f_q^{f_B=0}(q)\Theta(q - q_{\text{sh}}), \quad (15)$$

with coefficients c_{\pm} and d_{\pm} determined from the sum rule. We will relate k_{sh} and q_{sh} shortly, and it will turn out $k_{\text{sh}} = N_c q_{\text{sh}}$. The expression is valid for sufficiently small k_{sh} with which $f_q(0) \leq 1$. Beyond some value of k_{sh} , the extrapolation of Eq. (15) for large k_{sh} would violate the condition $f_q(0) \leq 1$. The saturation at $q = 0$ first occurs at $k_F \simeq \sqrt{2/N_c}\Lambda$ or $n_B/n_0 = 2.58 \times (\Lambda/0.4 \text{ GeV})^3$ for $N_c = 3$ ($n_0 \simeq 0.16 \text{ fm}^{-3}$: normal nuclear density). Note that this implies the saturation density is parametrically small compared to the QCD scale Λ^3 .

When quark states are filled at low momenta the solution should take the form

$$f_q(q) = \Theta(q_{\text{bu}} - q) + f_q^{f_B=1}(q)\Theta(q_{\text{sh}} - q)\Theta(q - q_{\text{bu}}) + f_q^{f_B=0}(q)\Theta(q - q_{\text{sh}}). \quad (16)$$

For $q \leq q_{\text{bu}}$ the quark states are saturated. Beyond $q \geq q_{\text{bu}}$ the quark distribution is dual to the saturated baryon distribution; here the baryons become free from the Pauli blocking constraint and hence f_B can take the maximal value 1. For $q \geq q_{\text{sh}}$, the quark distribution is dual to the baryon distribution where f_B is zero. Applying \hat{L} , we find

$$\frac{\Lambda^2}{N_c^d} \hat{L}[f_q(q)] = \frac{1}{N_c^d} \Theta(q_{\text{bu}} - q) + \Theta(q_{\text{sh}} - q)\Theta(q - q_{\text{bu}}) + \frac{\Lambda^2}{N_c^d} R, \quad (17)$$

where R comes from the application of derivatives on step functions,

$$R = [1 - f_q^{f_B=1}(q_{\text{bu}})]\delta'(q_{\text{bu}} - q) + [f_q^{f_B=1}(q_{\text{sh}}) - f_q^{f_B=0}(q_{\text{sh}})]\delta'(q_{\text{sh}} - q) - \nabla f_q^{f_B=1}(q_{\text{bu}})\delta(q - q_{\text{bu}}) + \nabla [f_q^{f_B=1}(q_{\text{sh}}) - f_q^{f_B=0}(q_{\text{sh}})]\delta(q - q_{\text{sh}}). \quad (18)$$

The function R would contain the δ - and δ' -functions which violate the condition $0 \leq f_B \leq 1$. This problem can be avoided by demanding f_q and df_q/dq to be continuous at each junction point. The resulting R vanishes and we get ($k = N_c q, k_{\text{bu}} = N_c q_{\text{bu}}, k_{\text{sh}} = N_c q_{\text{sh}}$)

$$f_B(k) = \frac{1}{N_c^d} \Theta(k_{\text{bu}} - k) + \Theta(k_{\text{sh}} - k)\Theta(k - k_{\text{bu}}). \quad (19)$$

The rest is the determination of k_{bu} that follows from the continuity conditions of f_q . This in turn requires the determination of c_{\pm} and d_{\pm} . One can set $c_+ = 0$ to satisfy $f_q \rightarrow 0$ for $q \rightarrow \infty$. So four conditions are sufficient to determine k_{bu} , c_- , and d_{\pm} .

With four conditions from two junction points, one can express c_- , d_{\pm} , and $\Delta_q = q_{\text{sh}} - q_{\text{bu}}$ as functions of q_{sh} . The conditions are

$$\begin{aligned} 1 &= f_q^{f_B=1}(q_{\text{bu}}), \\ 0 &= \frac{df_q^{f_B=1}(q_{\text{bu}})}{dq}, \\ f_q^{f_B=1}(q_{\text{sh}}) &= f_q^{f_B=0}(q_{\text{sh}}), \\ \frac{df_q^{f_B=1}(q_{\text{sh}})}{dq} &= \frac{df_q^{f_B=0}(q_{\text{sh}})}{dq}. \end{aligned} \quad (20)$$

the four coefficients are entirely determined by these four matching equations.

After lengthy calculations, the matching coefficients and Δ_q can be found as functions of q_{bu} and q_{sh} .

$$N_c^3 = \frac{\mathcal{X}_{N_c^3}}{\mathcal{Y}}, \quad d_+ = \frac{\mathcal{X}_{d_+}}{\mathcal{Y}}, \quad d_- = \frac{\mathcal{X}_{d_-}}{\mathcal{Y}}, \quad c_- = \frac{\mathcal{X}_{c_-}}{\mathcal{Y}}, \quad (21)$$

where the numerators are

$$\begin{aligned} \mathcal{X}_{N_c^3} &= -[y'_+(q_{\text{sh}})y_-(q_{\text{sh}}) - y_+(q_{\text{sh}})y'_-(q_{\text{sh}})]y'_-(q_{\text{bu}}), \\ \mathcal{X}_{d_+} &= -y'_-(q_{\text{bu}})y'_-(q_{\text{sh}}), \\ \mathcal{X}_{d_-} &= y'_+(q_{\text{bu}})y'_-(q_{\text{sh}}), \\ \mathcal{X}_{c_-} &= y'_+(q_{\text{bu}})y'_-(q_{\text{sh}}) - y'_-(q_{\text{bu}})y'_+(q_{\text{sh}}), \end{aligned} \quad (22)$$

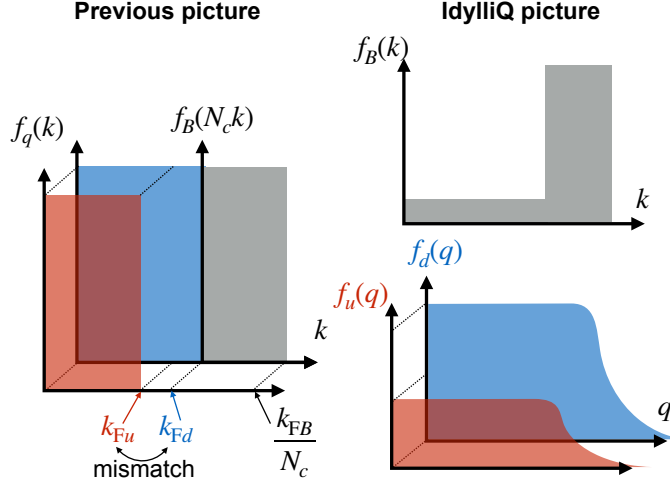


FIG. 1. Comparison of the previous model of Quarkyonic matter and IdylliQ model. In the previous picture, described by Eq. (29), there is a discrepancy between the Fermi momenta of u and d quarks, so the u -quark distribution has a mismatch with the nucleon distribution. Meanwhile, in the IdylliQ picture, this mismatch is naturally resolved by considering the half-occupied distribution for the u quark that is dual to the nucleonic description.

and the common denominator is

$$\mathcal{Y} = [y'_+(q_{\text{bu}})y_-(q_{\text{bu}}) - y_+(q_{\text{bu}})y'_-(q_{\text{bu}})]y'_-(q_{\text{sh}}) - [y'_+(q_{\text{sh}})y_-(q_{\text{sh}}) - y_+(q_{\text{sh}})y'_-(q_{\text{sh}})]y'_-(q_{\text{bu}}). \quad (23)$$

Here we display only the equation to determine Δ_q , which is obtained from the relation $N_c^3 = \mathcal{X}_{N_c^3}/\mathcal{Y}$; it is needed for the computations of EoS. The equation to be solved is

$$\frac{\Lambda + q_{\text{bu}}}{\Lambda + q_{\text{bu}} - (\Lambda + q_{\text{sh}})e^{-\Delta_q/\Lambda}} = N_c^3. \quad (24)$$

C. Comparison with the previous model of Quarkyonic Matter

Here, we show that the solution $f_B(k)$ for the IdylliQ model (17) leads to the same EoS as the one given in Ref. [38] based on the Fermi shell structure proposed in Ref. [32]. We also note in passing that, for systems with flavor asymmetry, there was a problematic mismatch between baryon Fermi momenta and quark Fermi momenta in the previous model of Quarkyonic matter [38] where quark occupation density is always assumed to be either 0 or 1. In the IdylliQ model, we allow the probability intermediate between 0 and 1, then this problem is automatically cured.

The EoS given in Ref. [38] are

$$n_B = 4 \int_{k_{\text{sh}} - \Delta}^{k_{\text{sh}}} \frac{d^3 \mathbf{k}}{(2\pi)^3} + \frac{4}{N_c^3} \int_0^{k_{\text{sh}} - \Delta} \frac{d^3 \mathbf{k}}{(2\pi)^3}, \quad (25)$$

$$\varepsilon = 4 \int_{k_{\text{sh}} - \Delta}^{k_{\text{sh}}} \frac{d^3 \mathbf{k}}{(2\pi)^3} \sqrt{k^2 + M_N} + \frac{4}{N_c^3} \int_0^{k_{\text{sh}} - \Delta} \frac{d^3 \mathbf{k}}{(2\pi)^3} \sqrt{k^2 + M_N}. \quad (26)$$

In the second integral in ε , we make the change of the variable $\mathbf{k} \rightarrow \mathbf{q} = \mathbf{k}/N_c$.

$$n_B = \frac{3}{2\pi^2} \left[k_{\text{sh}}^3 - (k_{\text{sh}} - \Delta)^3 + \frac{(k_{\text{sh}} - \Delta)^3}{N_c^3} \right], \quad (27)$$

$$\varepsilon = 4 \int_{k_{\text{sh}} - \Delta}^{k_{\text{sh}}} \frac{d^3 \mathbf{k}}{(2\pi)^3} \sqrt{k^2 + M_N^2} + 4N_c \int_0^{\frac{k_{\text{sh}} - \Delta}{N_c}} \frac{d^3 \mathbf{q}}{(2\pi)^3} \sqrt{q^2 + M_q^2}. \quad (28)$$

Note that $M_q = M_N/N_c$. After the change of the variable, the prefactor $1/N_c^3$ is canceled by the integration measure and an additional factor of N_c comes in from the kinetic energy. By relabeling k_{sh} and $(k_{\text{sh}} - \Delta)/N_c$ as k_{FB} and

k_{FQ} , respectively, these expressions of baryon density and energy density become exactly the same as Eqs. (3, 4) in Ref. [38]. The only difference is that in the IdylliQ model, the behavior of Δ is derived as a function of k_{sh} .

We showed that the form of the EoS is equivalent. Nevertheless, the IdylliQ model has the advantage since the origin of the baryon momentum shell structure is evident; the quark Pauli blocking constraint forces baryons to occupy high momenta. Also, the IdylliQ model does not use different degrees of freedom in different domains of the phase space and hence there is no worry about double counting. Exact counting of degrees of freedom becomes essential especially when we treat many baryon species, as we describe in the next section.

Now we mention that there is a problem with the mismatched Fermi momenta in the McLerran-Pisarski-Reddy model in the case of pure neutron matter, and this problem is naturally solved in the IdylliQ picture. In the previous studies, the energy density for the pure neutron matter with an asymmetry for u and d quarks are

$$\varepsilon = 2 \int_{k_{\text{sh}} - \Delta}^{k_{\text{sh}}} \frac{d^3 \mathbf{k}}{(2\pi)^3} \sqrt{k^2 + M_N^2} + 2 \sum_{\alpha=u,d} N_c \int_0^{k_{\text{F}\alpha}} \frac{d^3 \mathbf{q}}{(2\pi)^3} \sqrt{q^2 + M_q^2}, \quad (29)$$

where $k_{\text{F}d} = (k_{\text{sh}} - \Delta)/N_c$ and $k_{\text{F}u} = 2^{-1/3} k_{\text{F}d}$. At momenta less (larger) than these Fermi momenta, quark states are saturated (empty). The Fermi momentum for u quark $k_{\text{F}u}$ is smaller than $k_{\text{F}d}$, and they are unequal. While the lower bound of the neutron Fermi momenta is $k_{\text{sh}} - \Delta$, the upper bound for the u -quark Fermi momentum is $2^{-1/3}(k_{\text{sh}} - \Delta)/N_c$, so the upper bound and lower bound of the Fermi momentum do not match with each other for u quark sector. Such a large disparity between average quark momentum in neutrons and that of u -quark raises a question concerning the stability of neutrons near the Fermi surface; such neutrons would cost large energy or would be torn apart. The natural solution to this problem in the IdylliQ model is that the neutrons are still confined in the dual picture and this enforces the u -quark distribution to be half-occupied compared to the d -quark distribution. This natural explanation is an advantage of the IdylliQ description of Quarkyonic matter.

III. IDYLLIQ MODEL WITH MULTIPLE FLAVORS

In this section, we extend the IdylliQ model reviewed in the previous section to the case with multiple flavors. We determine the minimum energy solution in this setup by considering the chemical equilibrium condition, which constitutes the main result in this paper.

A. Simplified setup

Here we consider adding the hyperons (Y) with strangeness $S = -1$ on top of the neutron star matter in a very simplified setup. We approximate the baseline neutron star matter as pure neutron matter and neglect the contribution of protons and leptons. We only consider charge-neutral hyperons with strangeness $S = -1$ in the baryon octet, i.e., Λ^0 and Σ^0 . We assume the mass of Λ^0 and Σ^0 are degenerate, i.e., $M_Y \equiv M_{\Lambda^0} = M_{\Sigma^0}$, and we denote the degeneracy factor as $d_Y = 2$. We further consider the simplified setup in which all $S = -1$ hyperons are described by a single phase-space density distribution $f_Y(k) \equiv f_{\Lambda^0}(k) = f_{\Sigma^0}(k)$. By this simplification, electric charge neutrality is fulfilled within the baryonic sector. Therefore, we set the charge chemical potential to zero $\mu_Q = 0$.

The energy density described in terms of the momentum distribution of hadrons $f_i(k)$ ($i = n, Y$) is

$$\varepsilon = g \int_{\mathbf{k}} [E_N(k) f_n(k) + d_Y E_Y(k) f_Y(k)], \quad (30)$$

A factor $g = 2$ in front of the integral is the degeneracy of spins, and we use the ideal dispersion relation $E_i(k) = \sqrt{k^2 + M_i}$. The number density of neutrons and hyperons are

$$n_n = g \int_{\mathbf{k}} f_n(k), \quad n_Y = g \int_{\mathbf{k}} d_Y f_Y(k). \quad (31)$$

Another way to write this relation is in the basis of BSQ :

$$n_B = g \int_{\mathbf{k}} f_B(k), \quad f_B(k) = f_n(k) + d_Y f_Y(k), \quad (32)$$

$$n_S = g \int_{\mathbf{k}} f_S(k), \quad f_S(k) = -d_Y f_Y(k). \quad (33)$$

Note that the charge neutrality $n_Q = 0$ is fulfilled trivially as we only consider the charge-neutral combination of baryons.

Now, consider the momentum distribution of quarks: $f_q(q)$ ($q = u, d, s$). The confinement relation that sets the duality transformation between $f_B(k)$ and $f_q(q)$ is

$$f_q(q) = \sum_{i=n, \Sigma^0, \Lambda^0} \int_{\mathbf{k}} \varphi \left(\mathbf{q} - \frac{\mathbf{k}}{N_c} \right) B_q^i f_i(k), \quad (34)$$

where B_q^i is the baryon number carried by a quark of flavor q inside the baryon species i . We consider the case in which the d quark state saturates.

$$f_d(q) = \int_{\mathbf{k}} \varphi \left(\mathbf{q} - \frac{\mathbf{k}}{N_c} \right) [B_d^n f_n(k) + d_Y B_d^Y f_Y(k)], \quad (35)$$

$$f_u(q) = \int_{\mathbf{k}} \varphi \left(\mathbf{q} - \frac{\mathbf{k}}{N_c} \right) [B_u^n f_n(k) + d_Y B_u^Y f_Y(k)], \quad (36)$$

$$f_s(q) = \int_{\mathbf{k}} \varphi \left(\mathbf{q} - \frac{\mathbf{k}}{N_c} \right) [d_Y B_s^Y f_Y(k)], \quad (37)$$

where $B_d^n = 2/3$ and $B_d^Y = 1/3$ are the baryon number carried by constituent d quarks in neutrons and the average baryon number carried by constituent d quarks in hyperons. Also, $B_u^n = 1/3$ and $B_u^Y = 1/3$ for u quarks in baryons, and $B_s^Y = 1/3$ for s quarks in baryons. The low- k regions of $f_n(k)$ and $f_Y(k)$ are subject to the saturation of d -quark states $f_d(q)$ at $q \leq q_{\text{bu}}$. For baryons, the constraint is expressed as

$$B_d^n f_n^{\text{bulk}}(k) + d_Y B_d^Y f_Y^{\text{bulk}}(k) = \frac{1}{N_c^3}, \quad (38)$$

at $k \leq k_{\text{bu}} = N_c q_{\text{bu}}$. With the constraint, the f_n and f_Y are optimized to minimize the energy.

We consider the energy minimization with n_B fixed. As before we discuss how the particles with the maximal energy transform into particles with less energy. We assume that the shell part is saturated by neutrons while the bulk may be a mixture of neutrons and hyperons

$$f_n(k) = f_n^{\text{bulk}}(k) \Theta(k_{\text{bu}} - k) + \Theta(k - k_{\text{bu}}) \Theta(k_{\text{sh}} - k), \quad (39)$$

$$f_Y(k) = f_Y^{\text{bulk}}(k) \Theta(k_{\text{bu}} - k), \quad (40)$$

where $f_n^{\text{bulk}}(k)$ and $f_Y^{\text{bulk}}(k)$ satisfy the d -quark saturation condition Eq. (38). To optimize the composition in the bulk, we consider the conversion $n(k) \rightarrow Y(k)$ at $k < k_{\text{bu}}$. Here we have introduced the notation $B(k)$ which represents a baryon B with the magnitude of momentum being k .

B. Determination of the bulk composition

As done in Sec. II for isospin symmetric matter, we vary f_n and f_Y in the bulk to minimize the energy functional for a fixed n_B . A new element in this section is the saturation condition on the particle conversion processes. When one neutron converts into one hyperon, $n(k) \rightarrow Y(k)$, this opens the phase space for another hyperon to come to fill the state $Y(k)$, since neutrons contain two d -quarks while Σ^0, Λ^0 contain only single d -quark. This extra hyperon can be brought by the conversion of neutrons in the shell into hyperons in the bulk, $n(k_{\text{sh}}) \rightarrow Y(k)$. Through these sequences of the processes, not only the bulk but also the shell structure in momentum space are reorganized.

One can examine the energy gain and cost for each process while keeping n_B fixed. This can be manifestly done by varying f_n and f_Y as in Eq. (7). The calculations are rather lengthy and we postpone the step-by-step calculations to the Appendix C. Below, we show quicker calculations by focusing on the chemical equilibrium conditions.

The key observation to skip complications of number-conserving energy variation is that, when we reach the ground state, the conversion processes reach the equilibrium; knowing this fact allows us to impose the β -equilibrium condition from the very beginning for an efficient search for the ground state. We prepare several candidates of the solution (parametrization of f_n and f_Y), demand the β -equilibrium condition to fix the parameters in each candidate, and then single out the minimum solution at the same n_B .

For simplicity, we consider a sufficiently low density where hyperons have appeared. We can safely assume that those hyperons appear at low momenta with a constant occupation on the physical ground. Therefore, we take the

following ansatz for the solution:

$$f_n(k) = \frac{h_n}{N_c^3} \Theta(k_Y - k) \Theta(k) + \frac{1}{B_d^n N_c^3} \Theta(k - k_Y) \Theta(k_{\text{bu}} - k) + \Theta(k - k_{\text{bu}}) \Theta(k_{\text{sh}} - k), \quad (41)$$

$$f_Y(k) = \frac{h_Y}{N_c^3} \Theta(k_Y - k) \Theta(k). \quad (42)$$

From Eq. (38), the parameters h_n and h_Y satisfies

$$B_d^n h_n + d_Y B_d^Y h_Y = 1. \quad (43)$$

This implies that $0 \leq h_n \leq 1/B_d^n$ and $0 \leq h_Y \leq 1/(d_Y B_d^Y)$. Using these distributions and eliminating h_n by using Eq. (43) in the above equations, the thermodynamic quantities are

$$n_n/g = -d_Y \frac{h_Y}{N_c^3} \frac{B_d^Y}{B_d^n} \int_0^{k_Y} dk D(k) - \left(1 - \frac{1}{B_d^n N_c^3}\right) \int_0^{k_{\text{bu}}} dk D(k) + \int_0^{k_{\text{sh}}} dk D(k), \quad (44)$$

$$n_Y/g = d_Y \frac{h_Y}{N_c^3} \int_0^{k_Y} dk D(k), \quad (45)$$

$$\varepsilon/g = d_Y \frac{h_Y}{N_c^3} \int_0^{k_Y} dk D(k) \left[E_Y(k) - \frac{B_d^Y}{B_d^n} E_N(k) \right] - \left(1 - \frac{1}{B_d^n N_c^3}\right) \int_0^{k_{\text{bu}}} dk D(k) E_N(k) + \int_0^{k_{\text{sh}}} dk D(k) E_N(k), \quad (46)$$

where the density of states is given by $D(k) = k^2/(2\pi^2)$.

We have four parameters, h_Y, k_Y, k_{bu} , and k_{sh} . As we mentioned, we impose the β -equilibrium condition. The (candidates of) chemical potentials μ_n and μ_Y are given by

$$\mu_n = \left(\frac{\partial \varepsilon}{\partial n_n} \right)_{n_Y}, \quad \mu_Y = \left(\frac{\partial \varepsilon}{\partial n_Y} \right)_{n_n}. \quad (47)$$

The chemical potential for neutrons μ_n and μ_Y can be calculated by using the Jacobian. The details of calculations are given in Appendix A. The neutron chemical potential is found to be

$$\mu_n = \frac{-D(k_{\text{bu}}) E_N(k_{\text{bu}}) \left(1 - \frac{1}{B_d^n N_c^3}\right) \frac{\partial k_{\text{bu}}}{\partial k_{\text{sh}}} + D(k_{\text{sh}}) E_N(k_{\text{sh}})}{-D(k_{\text{bu}}) \left(1 - \frac{1}{B_d^n N_c^3}\right) \frac{\partial k_{\text{bu}}}{\partial k_{\text{sh}}} + D(k_{\text{sh}})}, \quad (48)$$

which is independent of hyperon parameters k_Y and h_Y ; it is essentially a function of k_{sh} as k_{bu} is fixed through the condition $f_n(k) = 1$ for $k_{\text{bu}} \leq k \leq k_{\text{sh}}$, in the similar way as Eq. (20). Meanwhile, the hyperon chemical potential is

$$\begin{aligned} \mu_Y &= E_Y(k_Y) - \frac{B_d^Y}{B_d^n} E_N(k_Y) + \frac{B_d^Y}{B_d^n} \mu_n \\ &= E_Y(k_Y) - \frac{1}{2} E_N(k_Y) + \frac{1}{2} \mu_n, \end{aligned} \quad (49)$$

where in the last line, we used $B_d^Y = 1/3$ and $B_d^n = 2/3$.

Now we demand $\mu_n = \mu_Y = \mu_B$. This condition can be understood as follows. The chemical potential of the baryon species i can be expressed in the BSQ basis as $\mu_i = B_i \mu_B + Q_i \mu_Q + S_i \mu_S$, where B_i, Q_i , and S_i are the baryon number, electric charge, and the strangeness of the baryon i , respectively. The β -equilibrium condition requires $\mu_S = 0$, and μ_Q is set to zero in our current setup.

Recalling that μ_n is a function of k_{sh} , the condition $\mu_n = \mu_Y = \mu_B$ turns into the relation between k_{sh} and k_Y for a given h_Y , which reads

$$\mu_B(k_{\text{sh}}) = 2E_Y(k_Y) - E_N(k_Y). \quad (50)$$

This is the necessary condition for the ground state. As we have derived the condition at a given h_Y , the parameters k_{sh} and k_Y should be regarded as functions of h_Y .

Finally, we determine h_Y by choosing the lowest energy solution out of candidates satisfying Eq. (50). The variation of h_n while holding n_B fixed yields

$$\left(\frac{\partial \varepsilon}{\partial h_Y} \right)_{n_B} = d_Y \frac{g}{N_c^3} \int_0^{k_Y} dk D(k) \left[E_Y(k) - \frac{1}{2} E_N(k) - \frac{1}{2} \mu_B \right]. \quad (51)$$

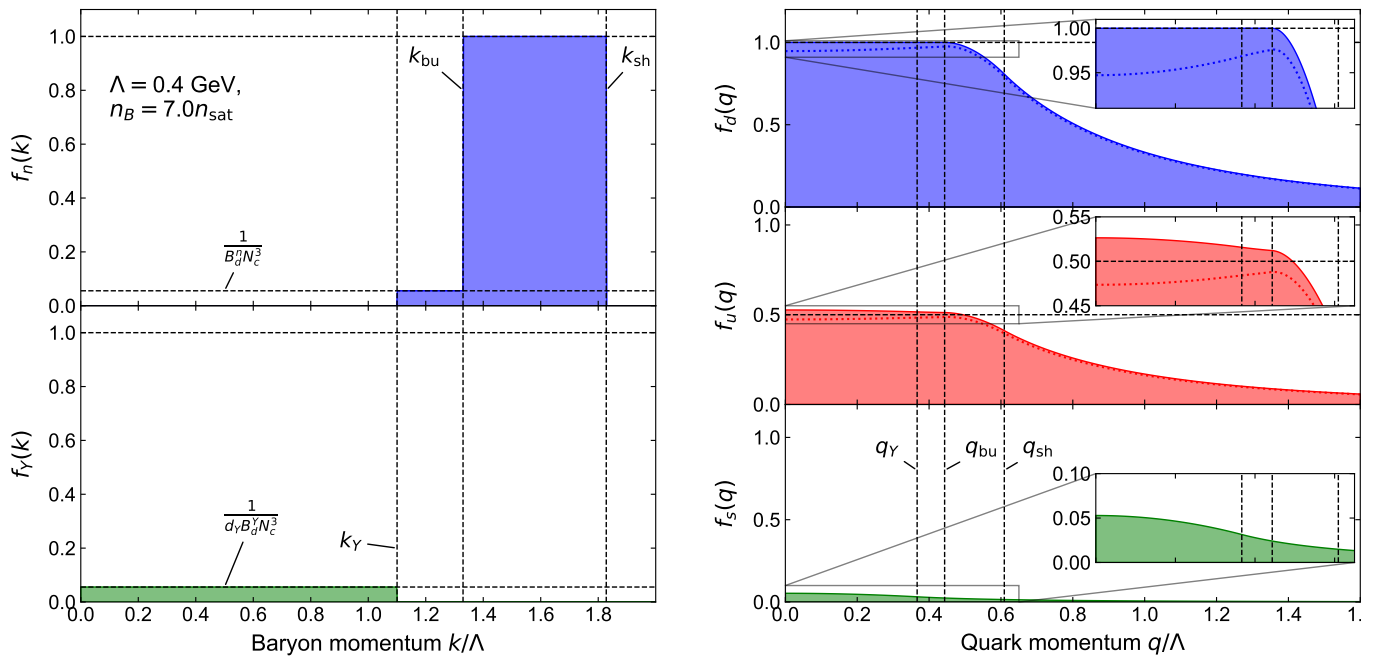


FIG. 2. Phase-space density distribution for baryons (left) and quarks (right).

We note that the integrand is a monotonically increasing function of k ,

$$\frac{\partial}{\partial k} [E_Y(k) - \frac{1}{2}E_N(k)] = \left(\frac{1}{E_Y(k)} - \frac{1}{2E_N(k)} \right) k > 0, \quad (52)$$

provided that $E_Y(k) < 2E_N(k)$. This condition holds for $M_Y < 2M_N$, valid for realistic baryon masses. Now we found that the integral is always negative for $k < k_Y$ and vanishes at $k = k_Y$, see Eq. (50). Therefore $(\partial\varepsilon/\partial h_Y)_{n_B} < 0$, favoring a larger h_Y . Consequently, h_Y takes the largest value possible; the domain of $k < k_Y$ is fully saturated by hyperons.

Now our solution takes the form

$$f_n(k) = \frac{1}{B_d^n N_c^3} \Theta(k - k_Y) \Theta(k_{bu} - k) + \Theta(k - k_{bu}) \Theta(k_{sh} - k), \quad (53)$$

$$f_Y(k) = \frac{1}{d_Y B_d^Y N_c^3} \Theta(k_Y - k). \quad (54)$$

with Eq. (50) for $h_Y = 1/(d_Y n_d^Y)$,

$$\mu_B = 2E_Y(k_Y) - E_N(k_Y). \quad (55)$$

The solution is valid for sufficiently large n_B . We recall that the RHS of Eq. (55) is an increasing function of k_Y so that μ_B at the onset of hyperons is

$$\mu_B^{\text{onset}} = 2M_Y - M_N, \quad (56)$$

below which it is not possible to satisfy the chemical equilibrium; neutrons completely dominate the system. A snapshot of the phase space distributions for baryons and quarks is shown in Fig. 2.

C. Equation of state

In Fig. 3, we show the EoS (44)-(46). The explicit expression of the EoS is given in Appendix B. The onset of hyperons is shown with dash-dotted lines in each figure.

There are two remarkable consequences of the quark saturation:

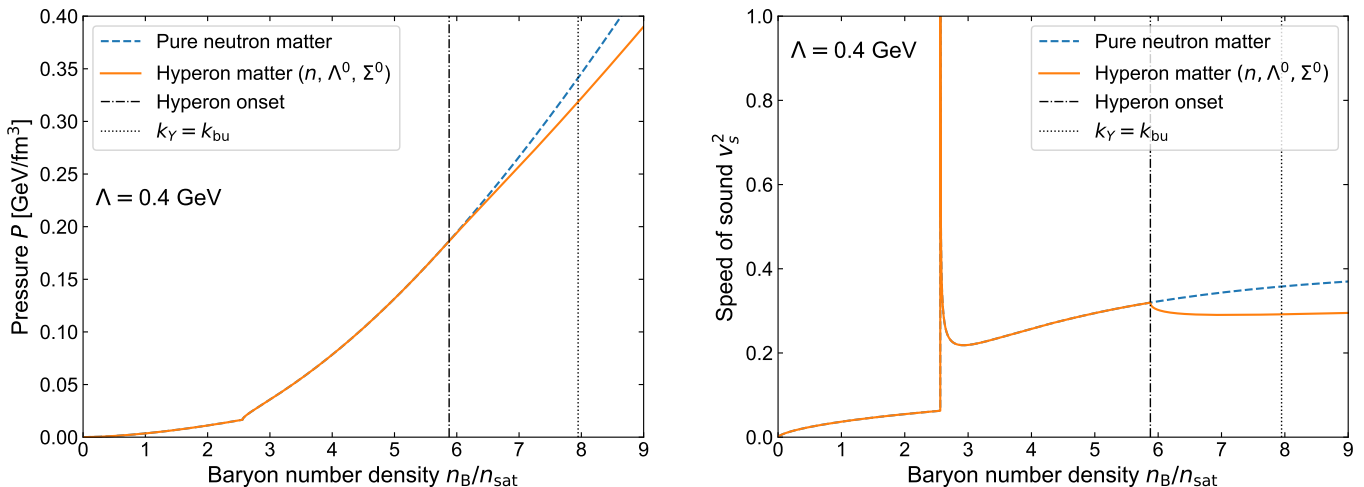


FIG. 3. Comparison of the equations of state between the pure neutron matter and the hyperon matter at $\Lambda = 0.4$ GeV. Left: Pressure as a function of n_B . Right: Speed of sound as a function of n_B .

First, hyperons emerge in the system at density $\sim (5-6)n_{\text{sat}}$, significantly higher than the usual estimate, $(2-3)n_{\text{sat}}$. We note that the typical core density of two-solar mass neutron stars is about $\sim 5n_0$; if our estimate on the hyperon onset is valid, the high mass is established before hyperons soften the EoS. Second, even after the appearance of hyperons, the softening is mild as the contribution of the hyperons is suppressed by a factor $1/N_c^3$. Since hyperons cannot largely occupy the phase space at low energy, increasing the hyperon density makes hyperons energetic more quickly than theories without the saturation; the relativistic regime for hyperons is reached at lower density.

We emphasize that all these dramatic effects arise solely from the statistical considerations, without any detailed discussions of interactions. We expect that the baryon-baryon interactions, which seem to be repulsive in most flavor channels, further stiffen the EoS.

Softening may be more significant when we add Ξ^0 , which is a heavier baryon not subject to d -quark saturation condition, and lies slightly above the threshold of hyperons with $S = -1$. This issue will be explained in the later section.

IV. DISCUSSION

In this section, we discuss several points regarding the solution we have given in the previous section. We consider adding heavier baryons. In particular, we consider Ξ^0 , which is a hyperon with strangeness $S = -2$, and Δ^0 , which is a baryon without strangeness in it whose mass lies between Σ^0 and Ξ^0 . We will see that the former has the same threshold as $S = -1$ hyperons while the latter turns out to be energetically disfavored and thus does not appear in the current setup. Then, we mention the applicable limit of our current solution, and close with the possible future direction.

A. Including heavier baryons: the case of Ξ^0

Now we consider including the heavier baryons. Among the charge-neutral hyperons, the quark content of Ξ^0 is uss , so the threshold is never affected by the d -quark saturation effect. In additive quark models, the threshold is estimated to be

$$(\mu_B)_{\text{onset}}^{\Xi^0} = M_{\Xi^0} \sim 2M_s + M_u, \quad (57)$$

where M_{Ξ^0} is the mass of Ξ^0 which is close to the onset of Λ^0 and Σ^0 ,

$$(\mu_B)_{\text{onset}}^{\Lambda^0, \Sigma^0} = 2M_Y - M_N \sim 2M_s + M_u. \quad (58)$$

Therefore, at the threshold of hyperons with $S = -1$, the cascade baryon Ξ^0 with $S = -2$ also enters the system. Below, for simplicity, we approximate M_{Ξ^0} to $2M_Y - M_N$ and discuss the effect of Ξ^0 to the EoS.

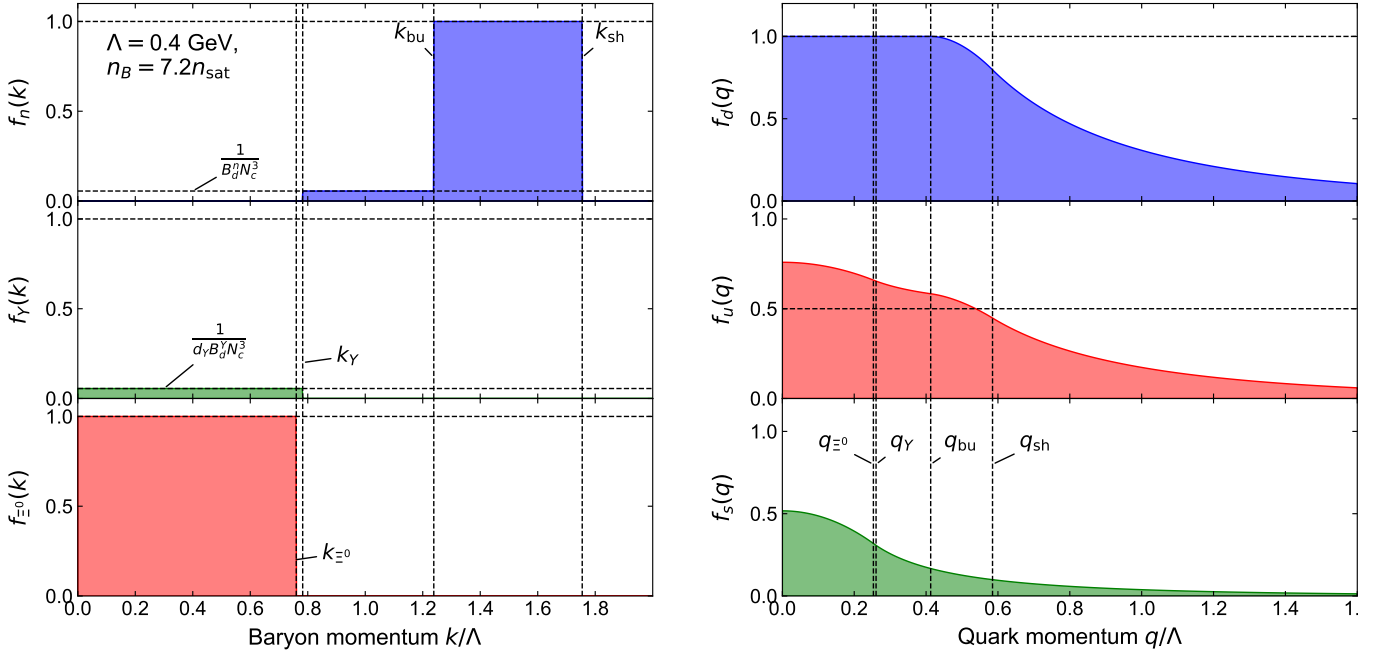


FIG. 4. Phase-space density distribution for baryons (left) and quarks (right).

As Ξ^0 is never affected by the d -quark saturation condition, momentum distribution is given by

$$f_{\Xi^0}(k) = \Theta(k_{\Xi^0} - k), \quad (59)$$

where k_{Ξ^0} is the Fermi momentum of Ξ^0 baryon, $k_{\Xi^0} = \sqrt{\mu_B^2 - M_{\Xi^0}^2}$. In Fig. 4, we plot the phase-space distribution for baryons and quarks in the corresponding dual picture. From this distribution, the number density of Ξ^0 and the total energy density become

$$n_{\Xi^0}/g = \int_0^{k_{\Xi^0}} dk D(k), \quad (60)$$

$$\begin{aligned} \varepsilon/g &= \frac{1}{N_c^3} \int_0^{k_Y} dk D(k) \left[\frac{E_Y(k)}{B_d^Y} - \frac{E_N(k)}{B_d^N} \right] - \left(1 - \frac{1}{B_d^N N_c^3} \right) \int_0^{k_{bu}} dk D(k) E_N(k) + \int_0^{k_{sh}} dk D(k) E_N(k) \\ &\quad + \int_0^{k_{\Xi^0}} dk D(k) E_{\Xi^0}(k), \end{aligned} \quad (61)$$

where $E_{\Xi^0}(k) = \sqrt{k^2 + M_{\Xi^0}^2}$ represents the energy dispersion relation for Ξ^0 . We find the chemical potential is

$$\mu_{\Xi^0} = \left(\frac{\partial \varepsilon}{\partial n_{\Xi^0}} \right)_{n_n, n_Y} = E_{\Xi^0}(k_{\Xi^0}). \quad (62)$$

The β -equilibrium condition implies $\mu_B = \mu_{\Xi^0}$, and this relation determines the value of k_{Ξ^0} at a given μ_B .

Shown in Fig. 5 is the EoS including Ξ^0 . We see the radical softening above the hyperon onset. But this softening regime ends soon as u - or s -quarks get saturated within a small density interval. The computations of u - and s -quark saturation will be presented elsewhere.

B. Including heavier baryons: the case of Δ^0

Here, we discuss that Δ^0 , which is another charge-neutral baryon lighter than Ξ^0 , does not appear in this setup from the vantage point of energetics. One can compute the chemical potential for Δ^0 from the relation $\mu_{\Delta^0} =$

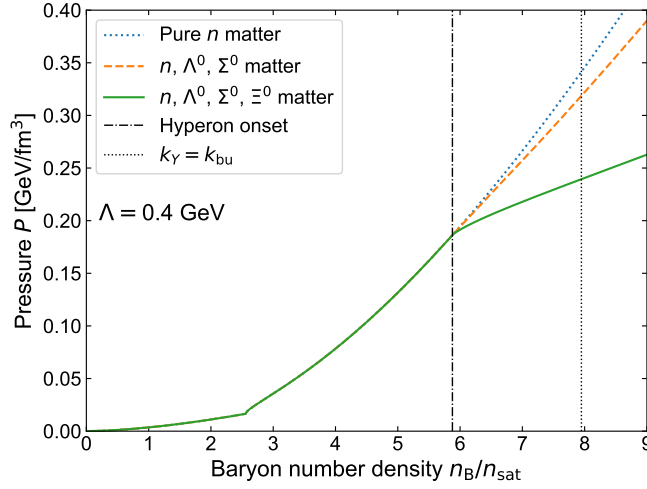


FIG. 5. Comparison of the energy density at a given baryon density among the pure neutron matter, the $S = -1$ hyperon matter, and the hyperon matter with Ξ^0 .

$(\partial\varepsilon/\partial n_{\Delta^0})_{n_n, n_Y}$:

$$\begin{aligned}\mu_{\Delta^0} &= E_{\Delta^0}(k_{\Delta^0}) - \frac{B_d^{\Delta^0}}{B_d^Y} E_Y(k_{\Delta^0}) + \frac{B_d^{\Delta^0}}{B_d^Y} \mu_Y, \\ &= E_{\Delta^0}(k_{\Delta^0}) - 2E_Y(k_{\Delta^0}) + 2\mu_Y,\end{aligned}\quad (63)$$

where k_{Δ^0} is the Fermi momentum of Δ^0 and $B_d^{\Delta^0} = 2/3$ is the baryon number carried by d quarks inside the Δ^0 baryon. As one can explicitly verify, the value of the chemical potential is independent of h_{Δ^0} . Therefore, one can set the β -equilibrium condition regardless of the value of h_{Δ^0} . In the β -equilibrium, one finds $\mu_Y = \mu_B$ and $\mu_{\Delta^0} = \mu_B$.

The variation of the energy with respect to h_{Δ^0} reads

$$\begin{aligned}\left(\frac{\partial\varepsilon}{\partial h_{\Delta^0}}\right)_{n_B} &= d_{\Delta^0} \frac{g}{N_c^3} \int_0^{k_{\Delta^0}} dk D(k) \left[E_{\Delta^0}(k) - \frac{B_d^{\Delta^0}}{B_d^Y} E_Y(k) - \left(1 - \frac{B_d^{\Delta^0}}{B_d^Y}\right) \mu_B \right], \\ &= d_{\Delta^0} \frac{g}{N_c^3} \int_0^{k_{\Delta^0}} dk D(k) [E_{\Delta^0}(k) - 2E_Y(k) + \mu_B] > 0.\end{aligned}\quad (64)$$

One can easily verify that the integrand is positive for $k < k_{\Delta^0}$. From this argument, one can say that $h_{\Delta^0} = 0$ is the minimum energy solution. This means that the appearance of the Δ^0 baryons is disfavored in this setup.

C. Applicability of the solution

The aforementioned solution is valid when the following four conditions are fulfilled: (i) $\Lambda \lesssim 740$ MeV. (ii) $k_Y < k_{bu}$. (iii) $f_u(q) < 1$ and $f_s(q) < 1$ for any q . (iv) $\mu_B \lesssim N_c^{3/2} \Lambda_{\text{QCD}}$.

First, the ansatz for f_n and f_Y (41, 42) is valid as long as the saturation of the d -quark distribution occurs at $\mu_B < M_Y$. When $k_{sh}^Y \equiv \sqrt{\mu_B^2 - M_Y^2}$ exceeds k_{bu} , neutrons at k_{sh} can decay into hyperons with the momentum $k_{sh}^Y (\geq k_{bu})$. Removing a neutron at k_{sh} reorganizes the shell structure and reduces the energy by $\mu_B (> E_n(k_{sh}))$, and the baryon number conservation demands the system to accommodate another baryon. Adding a hyperon in the shell domain costs at least the energy of $\sqrt{M_Y^2 + k_{bu}^2}$. When the conversion of neutrons to hyperons within the shell is energetically preferred, the $S = -1$ hyperons also develop the shell structure like in the neutron distribution. Such a situation may be realized when Λ is large and the saturation of the quark distribution occurs at low μ_B . It occurs when $\Lambda \simeq 740$ MeV or larger. This is derived from the Fermi momentum at which the saturation of the d -quark distribution occurs $k_{sat} \sim (2/N_c)^{1/2} \Lambda$, and the condition that the d -quark distribution saturates below the hyperon onset $\mu_{sat} = \sqrt{k_{sat}^2 + M_N^2} > M_Y$.

Secondly, when k_Y exceeds k_{bu} , the solution (53, 54) is no longer valid. One has to also consider the shell structure in $S = -1$ hyperon distribution f_Y as in the neutron distribution. This applicable limit is plotted with the dotted lines in Figs. 3, 5.

Thirdly, when the u and s quark distributions, $f_u(q)$ and $f_s(q)$, are saturated, the Ξ^0 hyperon will also have the low occupation at low momentum and the shell structure at high momentum. Such a situation demands us to manifestly consider u - or s -quark saturation conditions. We note that, once either u - or s -quark states are saturated together with d -quarks, no baryon octet can be free from the saturation conditions; all baryon octets are suppressed at low momenta.

Finally, when $\mu_B \gtrsim N_c^{3/2} \Lambda_{\text{QCD}}$, the color screening suppresses the confining gluons so that Quarkyonic picture may no longer be valid.

D. Toward a more realistic neutron-star equation of state

In this paper, we have modeled the neutron star matter with only the charge-neutral baryons, and there are two important effects we have neglected here: the lepton contribution and the interaction.

Regarding the first point, a neutron star in reality is composed not only of strongly interacting particles but of leptons as well. The charge neutrality condition together with the β -equilibrium introduces a certain fraction of protons and leptons. Since the chemical potential of leptons is finite in such a realistic environment, the chemical potential for the charged baryon can be modified. Therefore, the threshold for the negatively charged baryons may be shifted to lower density by the charge chemical potential μ_Q . Nevertheless, the shift in the hyperon threshold in this paper holds regardless of whether there is a finite μ_Q . As long as the d -quark states are saturated, there is a systematic shift in the threshold, and such shift is of the order of ~ 0.1 GeV while the effect of μ_Q may be of the order of ~ 0.01 GeV. So, even if μ_Q is nonzero, which can lower the charged hyperon threshold, the picture we have presented in this paper remains intact.

Regarding the second point, although we have taken into account some fraction of the interaction by taking into account the confinement effect, essentially the low-energy neutrons are treated as an ideal gas, at which the effect of the interaction is shown to be already important. The interaction may be modeled simply by the excluded volume effect [39, 48] as in the van-der-Waals EoS [49, 50]. Work in these directions is in progress.

ACKNOWLEDGMENTS

YF and TK would like to thank the Yukawa Institute for Theoretical Physics at Kyoto University and RIKEN iTHEMS, where part of this work was completed during the International Molecule-type Workshop ‘‘Condensed Matter Physics of QCD 2024’’ (YITP-T-23-05). The work of YF and LM was supported by the Institute for Nuclear Theory’s U.S. DOE Grant No. DE-FG02-00ER41132. YF is supported by Japan Science and Technology Agency (JST) as part of Adopting Sustainable Partnerships for Innovative Research Ecosystem (ASPIRE), Grant No. JPMJAP2318. TK is supported by JSPS KAKENHI Grant No. 23K03377 and No. 18H05407 and by the Graduate Program on Physics for the Universe (GPPU) at Tohoku University.

Appendix A: Details of calculations using Jacobian

Here, we give details of calculations using Jacobian for derivatives that appear in the main text.

We first take up the computation of neutron chemical potential. We take the derivative of energy density holding n_Y fixed. It can be written

$$\mu_n = \left(\frac{\partial \varepsilon}{\partial n_n} \right)_{n_Y} = \frac{\partial(\varepsilon, n_Y)}{\partial(n_n, n_Y)} = \frac{\partial(\varepsilon, n_Y)}{\partial(k_{\text{sh}}, k_Y)} \bigg/ \frac{\partial(n_n, n_Y)}{\partial(k_{\text{sh}}, k_Y)}. \quad (\text{A1})$$

Each determinant reads

$$\frac{\partial(\varepsilon, n_Y)}{\partial(k_{\text{sh}}, k_Y)} = \left(\frac{\partial \varepsilon}{\partial k_{\text{sh}}} \right)_{k_Y} \left(\frac{\partial n_Y}{\partial k_Y} \right)_{k_{\text{sh}}} - \left(\frac{\partial \varepsilon}{\partial k_Y} \right)_{k_{\text{sh}}} \left(\frac{\partial n_Y}{\partial k_{\text{sh}}} \right)_{k_Y}, \quad (\text{A2})$$

and

$$\frac{\partial(n_n, n_Y)}{\partial(k_{\text{sh}}, k_Y)} = \left(\frac{\partial n_n}{\partial k_{\text{sh}}} \right)_{k_Y} \left(\frac{\partial n_Y}{\partial k_Y} \right)_{k_{\text{sh}}} - \left(\frac{\partial n_n}{\partial k_Y} \right)_{k_{\text{sh}}} \left(\frac{\partial n_Y}{\partial k_{\text{sh}}} \right)_{k_Y}. \quad (\text{A3})$$

Noting $(\partial n_Y / \partial k_{\text{sh}})_{k_Y} = 0$ since holding k_Y and h_Y fixed does not change n_Y , we find

$$\mu_n = \left(\frac{\partial \varepsilon}{\partial k_{\text{sh}}} \right)_{k_Y} / \left(\frac{\partial n_n}{\partial k_{\text{sh}}} \right)_{k_Y}. \quad (\text{A4})$$

Explicitly,

$$\left(\frac{\partial \varepsilon}{\partial k_{\text{sh}}} \right)_{k_Y} = -D(k_{\text{bu}})E_N(k_{\text{bu}}) \left(1 - \frac{1}{B_d^n N_c^3} \right) \frac{\partial k_{\text{bu}}}{\partial k_{\text{sh}}} + D(k_{\text{sh}})E_N(k_{\text{sh}}), \quad (\text{A5})$$

$$\left(\frac{\partial n_n}{\partial k_{\text{sh}}} \right)_{k_Y} = -D(k_{\text{bu}}) \left(1 - \frac{1}{B_d^n N_c^3} \right) \frac{\partial k_{\text{bu}}}{\partial k_{\text{sh}}} + D(k_{\text{sh}}). \quad (\text{A6})$$

The chemical potential for hyperons μ_Y can be computed in the same way,

$$\begin{aligned} \mu_Y &= \frac{\partial(\varepsilon, n_n)}{\partial(k_{\text{sh}}, k_Y)} / \frac{\partial(n_Y, n_n)}{\partial(k_{\text{sh}}, k_Y)} \\ &= \frac{\left(\frac{\partial \varepsilon}{\partial k_Y} \right)_{k_{\text{sh}}}}{\left(\frac{\partial n_Y}{\partial k_Y} \right)_{k_{\text{sh}}}} - \frac{\left(\frac{\partial n_n}{\partial k_Y} \right)_{k_{\text{sh}}}}{\left(\frac{\partial n_Y}{\partial k_Y} \right)_{k_{\text{sh}}}} \mu_n, \end{aligned} \quad (\text{A7})$$

where

$$\left(\frac{\partial \varepsilon}{\partial k_Y} \right)_{k_{\text{sh}}} = g d_Y \frac{h_Y}{N_c^3} D(k_Y) \left[E_Y(k_Y) - E_N(k_Y) \frac{B_d^Y}{B_d^n} \right], \quad (\text{A8})$$

$$\left(\frac{\partial n_Y}{\partial k_Y} \right)_{k_{\text{sh}}} = g d_Y \frac{h_Y}{N_c^3} D(k_Y), \quad (\text{A9})$$

$$\left(\frac{\partial n_n}{\partial k_Y} \right)_{k_{\text{sh}}} = -g d_Y \frac{B_d^Y}{B_d^n} \frac{h_Y}{N_c^3} D(k_Y). \quad (\text{A10})$$

Using these we obtain the chemical potentials in the main text:

$$\mu_n = \frac{-D(k_{\text{bu}})E_N(k_{\text{bu}}) \left(1 - \frac{1}{B_d^n N_c^3} \right) \frac{\partial k_{\text{bu}}}{\partial k_{\text{sh}}} + D(k_{\text{sh}})E_N(k_{\text{sh}})}{-D(k_{\text{bu}}) \left(1 - \frac{1}{B_d^n N_c^3} \right) \frac{\partial k_{\text{bu}}}{\partial k_{\text{sh}}} + D(k_{\text{sh}})}, \quad (\text{A11})$$

$$\mu_Y = E_Y(k_Y) - \frac{B_d^Y}{B_d^n} E_N(k_Y) + \frac{B_d^Y}{B_d^n} \mu_n. \quad (\text{A12})$$

Next we compute the derivative of ε with respect to h_Y for a fixed n_B :

$$\begin{aligned} \left(\frac{\partial \varepsilon}{\partial h_Y} \right)_{n_B} &= \frac{\partial(\varepsilon, n_B)}{\partial(h_Y, n_B)} = \frac{\partial(\varepsilon, n_B)}{\partial(h_Y, k_{\text{sh}})} / \frac{\partial(n_B, n_B)}{\partial(h_Y, k_{\text{sh}})} \\ &= \frac{\left(\frac{\partial \varepsilon}{\partial h_Y} \right)_{k_{\text{sh}}} \left(\frac{\partial n_B}{\partial k_{\text{sh}}} \right)_{h_Y} - \left(\frac{\partial n_B}{\partial h_Y} \right)_{k_{\text{sh}}} \left(\frac{\partial \varepsilon}{\partial k_{\text{sh}}} \right)_{h_Y}}{\left(\frac{\partial n_B}{\partial k_{\text{sh}}} \right)_{h_Y}} \\ &= \left(\frac{\partial \varepsilon}{\partial h_Y} \right)_{k_{\text{sh}}} - \left(\frac{\partial n_B}{\partial h_Y} \right)_{k_{\text{sh}}} \left(\frac{\partial \varepsilon}{\partial n_B} \right)_{h_Y} \\ &= d_Y \frac{g}{N_c^3} \int_0^{k_Y} dk D(k) \left[E_Y(k) - \frac{B_d^Y}{B_d^n} E_N(k) - \left(1 - \frac{B_d^Y}{B_d^n} \right) \mu_B \right]. \end{aligned} \quad (\text{A13})$$

Appendix B: Expression of the equation of state

The equation of state (EoS) is always a function of the Fermi momentum k_{sh} . Below the hyperon threshold, the EoS is described by the pure neutron matter with the low momentum part of the d quark states saturated. Above the hyperon threshold, the EoS is a mixture of neutrons and degenerate hyperons.

a. *Below the saturation and below the hyperon threshold*

The EoS is that of an ideal gas in this regime:

$$n_B = g \frac{k_{\text{sh}}^3}{6\pi^2}, \quad (\text{B1})$$

$$\varepsilon = g e_3(k_{\text{sh}}, M_N), \quad (\text{B2})$$

$$\mu_B = \sqrt{k_{\text{sh}}^2 + M_N^2}, \quad (\text{B3})$$

where the function e_3 is defined as

$$e_3(k, M) = \int_0^k dx D(x) \sqrt{k^2 + M^2} = \frac{1}{16\pi^2} k \sqrt{k^2 + M^2} (2k^2 + M^2) + \frac{1}{16\pi^2} M^4 \ln \left(\frac{\sqrt{k^2 + M^2} - k}{M} \right). \quad (\text{B4})$$

b. *Saturation condition for pure neutron matter*

The saturation takes place when $f_d(q=0) = 1$. This happens when

$$f_d(q=0) = B_d^n N_c^3 \left[1 - e^{-k_{\text{sh}}/(N_c \Lambda)} \left(1 + \frac{k_{\text{sh}}}{N_c \Lambda} \right) \right]. \quad (\text{B5})$$

c. *Above the saturation and below the hyperon threshold*

Above the saturation, one has to solve the equation to obtain the shell thickness Δ or the fermi momentum for the under-occupied bulk part $k_{\text{bu}} = k_{\text{sh}} - \Delta$. The equation is

$$\frac{N_c \Lambda + k_{\text{sh}} - \Delta}{N_c \Lambda + k_{\text{sh}} - \Delta - (N_c \Lambda + k_{\text{sh}}) e^{-\Delta/(N_c \Lambda)}} = B_d^n N_c^3. \quad (\text{B6})$$

Then, from Δ determined above, the EoS is obtained as

$$n_B = -g \left(1 - \frac{1}{B_d^n N_c^3} \right) \frac{k_{\text{bu}}^3}{6\pi^2} + g \frac{k_{\text{sh}}^3}{6\pi^2}, \quad (\text{B7})$$

$$\varepsilon = -g \left(1 - \frac{1}{B_d^n N_c^3} \right) e_3(k_{\text{bu}}, M_N) + g e_3(k_{\text{sh}}, M_N), \quad (\text{B8})$$

$$\begin{aligned} \mu_B &= \frac{-k_{\text{bu}}^2 E_N(k_{\text{bu}}) \left(1 - \frac{1}{B_d^n N_c^3} \right) \frac{\partial k_{\text{bu}}}{\partial k_{\text{sh}}} + k_{\text{sh}}^2 E_N(k_{\text{sh}})}{-k_{\text{bu}}^2 \left(1 - \frac{1}{B_d^n N_c^3} \right) \frac{\partial k_{\text{bu}}}{\partial k_{\text{sh}}} + k_{\text{sh}}^2} \\ &= \frac{-k_{\text{bu}}(N_c \Lambda + k_{\text{bu}}) E_N(k_{\text{bu}}) \left(1 - \frac{1}{B_d^n N_c^3} \right) + k_{\text{sh}} E_N(k_{\text{sh}}) (N_c \Lambda + k_{\text{sh}})}{-k_{\text{bu}}(N_c \Lambda + k_{\text{bu}}) \left(1 - \frac{1}{B_d^n N_c^3} \right) + k_{\text{sh}} (N_c \Lambda + k_{\text{sh}})}, \end{aligned} \quad (\text{B9})$$

where in the last line, we use the relation

$$\frac{\partial \Delta}{\partial k_{\text{sh}}} = - \frac{N_c \Lambda \Delta}{(N_c \Lambda + k_{\text{sh}})(k_{\text{sh}} - \Delta)}, \quad (\text{B10})$$

$$\frac{\partial k_{\text{bu}}}{\partial k_{\text{sh}}} = 1 - \frac{\partial \Delta}{\partial k_{\text{sh}}} = \frac{k_{\text{sh}}(N_c \Lambda + k_{\text{sh}} - \Delta)}{(N_c \Lambda + k_{\text{sh}})(k_{\text{sh}} - \Delta)}. \quad (\text{B11})$$

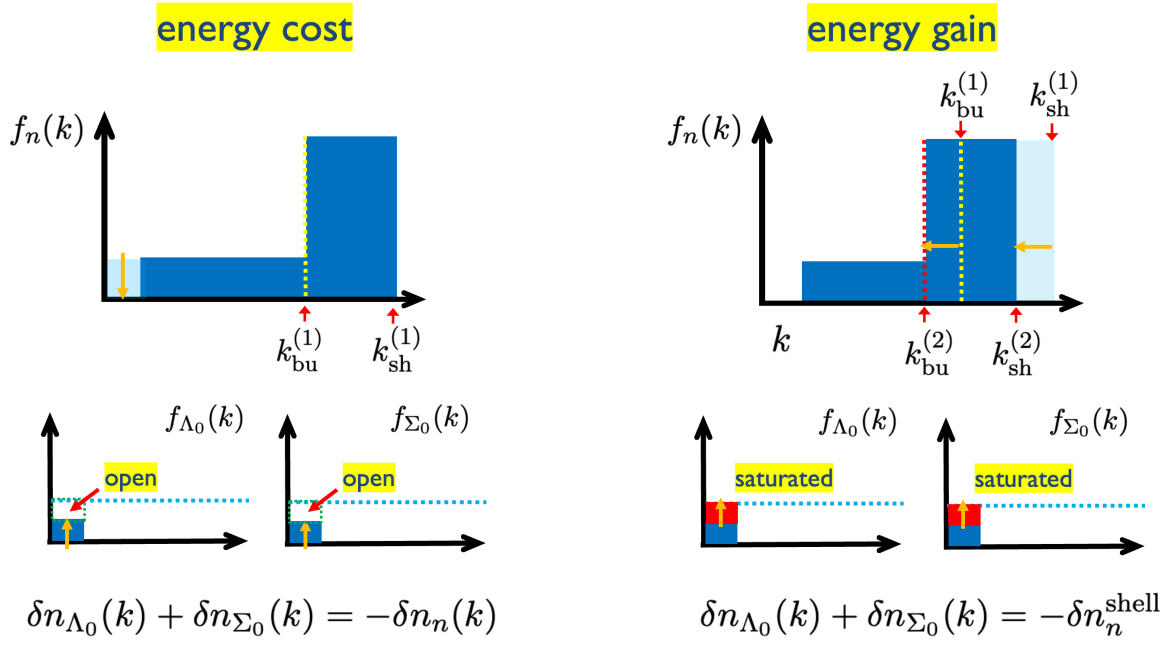


FIG. 6. Compositional changes initiated with the conversion of neutrons into hyperons which in turn triggers structural changes in the neutron momentum shell. The d -quark states are saturated at low momenta before and after these processes. Each conversion process conserves the baryon number. (Left) Neutrons at the momenta k transform into Λ^0 or Σ^0 , $n(k) \rightarrow \Lambda(k)$ or $\Sigma^0(k)$ with the energetic cost. Hyperons contain fewer d -quarks than neutrons so that the conversion $n \rightarrow Y$ in the bulk leaves the phase space open for d -quarks or other hyperons; (Right) The open phase space is filled by hyperons converted from neutrons in the shell. This process continues until d -quark states get saturated. Removing the baryon number from the shell, the shell structure is reorganized by reducing k_{sh} and k_{bu} as $k_{bu}^{(1)} \rightarrow k_{bu}^{(2)}$ and $k_{sh}^{(1)} \rightarrow k_{sh}^{(2)}$. This conversion reduces the energy of the system. Although we show these processes sequentially, they can occur at once. Whether the energy of the system decreases or not depends on the value of k .

d. Above the saturation and above the hyperon threshold

After the d -quark saturation occurs and μ_B exceeds the hyperon threshold, the EoS are

$$n_B = \frac{g}{N_c^3} \left(\frac{1}{B_d^Y} - \frac{1}{B_d^n} \right) \frac{k_Y^3}{6\pi^2} - g \left(1 - \frac{1}{B_d^n N_c^3} \right) \frac{k_{bu}^3}{6\pi^2} + g \frac{k_{sh}^3}{6\pi^2}, \quad (\text{B12})$$

$$n_S = -\frac{g}{B_d^Y N_c^3} \frac{k_Y^3}{6\pi^2}, \quad (\text{B13})$$

$$\varepsilon = \frac{g}{N_c^3} \left[\frac{e_3(k_Y, M_Y)}{B_d^Y} - \frac{e_3(k_Y, M_N)}{B_d^n} \right] - g \left(1 - \frac{1}{B_d^n N_c^3} \right) e_3(k_{bu}, M_N) + g e_3(k_{sh}, M_N), \quad (\text{B14})$$

$$\mu_B = \frac{-k_{bu}(N_c \Lambda + k_{bu}) E_N(k_{bu}) \left(1 - \frac{1}{B_d^n N_c^3} \right) + k_{sh} E_N(k_{sh}) (N_c \Lambda + k_{sh})}{-k_{bu}(N_c \Lambda + k_{bu}) \left(1 - \frac{1}{B_d^n N_c^3} \right) + k_{sh} (N_c \Lambda + k_{sh})}, \quad (\text{B15})$$

And the k_Y is determined through the β -equilibrium condition

$$\mu_B = 2E_Y(k_Y) - E_N(k_Y). \quad (\text{B16})$$

Appendix C: Stepwise minimization with fixed baryon density

In this appendix we consider the variation of energy, manifestly holding n_B fixed. We consider the conversion of $n(k) \rightarrow Y(k)$ for baryons with momentum $k \leq k_{bu}$ and subsequent modification of the shell. The advantage of this strategy is that one can identify which processes cost and gain the energy, see Fig. 6.

We first consider the process $n(k) \rightarrow \Lambda^0(k)$ or $\Sigma^0(k)$. The variation of each density at momentum k is

$$\delta n_n(k) + \delta n_{\Lambda^0}^{(1)}(k) + \delta n_{\Sigma^0}^{(1)}(k) = 0, \quad (\text{C1})$$

where we defined

$$\delta n_i(k) \equiv \delta f_i(k) D(k) dk, \quad (\text{C2})$$

with $D(k) = k^2/2\pi^2$ being the density of states at k . Assuming Λ^0 and Σ^0 are generated at equal probability, in this first conversion process the density of each hyperon species changes as

$$\delta n_Y^{(1)}(k) \equiv \delta n_{\Lambda^0}^{(1)}(k) = \delta n_{\Sigma^0}^{(1)}(k) = -\frac{\delta n_n(k)}{2}. \quad (\text{C3})$$

After this conversion, the d -quarks are no longer saturated. This is because we lose a single d -quark for each $n(k; udd) \rightarrow Y(k; uds)$ process. We also note that this first process costs the energy $E_Y(k) - E_n(k)$ for each conversion and never occurs unless the new energy reduction process becomes possible by this conversion.

To fill the hole in the d -quark states in the bulk, we consider the second conversion process in which the neutrons in the shell decay into hyperons in the bulk. In this second process, the hyperon densities increase until the d -quark states are saturated,

$$\delta n_Y^{(2)}(k) = \delta n_{\Lambda^0}^{(2)}(k) = \delta n_{\Sigma^0}^{(2)}(k) = \delta n_Y^{(1)}(k). \quad (\text{C4})$$

Thus, the amount of decaying neutrons is

$$-\delta n_n^{\text{shell}} = \delta n_{\Lambda^0}^{(2)}(k) + \delta n_{\Sigma^0}^{(2)}(k) = -\delta n_n(k). \quad (\text{C5})$$

Reducing the number of neutrons in the shell, the shell structure is reorganized until the optimized (saturated) distribution is achieved again. As we have explicitly calculated in isospin symmetric matter, the momenta k_{bu} and k_{sh} for the saturated momentum shell are uniquely related. The k_{bu} and k_{sh} before (index 1) and after (index 2) satisfy the relation

$$F_{\text{sat}}(k_{\text{bu}}^{(1)}, k_{\text{sh}}^{(1)}) = F_{\text{sat}}(k_{\text{bu}}^{(2)}, k_{\text{sh}}^{(2)}) = 0. \quad (\text{C6})$$

and hence the relation between $dk_{\text{bu}} = k_{\text{bu}}^{(2)} - k_{\text{bu}}^{(1)} (< 0)$ and $dk_{\text{sh}} = k_{\text{sh}}^{(2)} - k_{\text{sh}}^{(1)} (< 0)$ is also uniquely specified. Now we can write the variation of neutron number in the shell as

$$\delta n_n^{\text{shell}} = -\left(1 - \frac{1}{B_d^n N_c^3}\right) D(k_{\text{bu}}) dk_{\text{bu}} + D(k_{\text{sh}}) dk_{\text{sh}}. \quad (\text{C7})$$

Here we assumed that the bulk just below k_{bu} is saturated by neutrons; in the interval $[k_{\text{bu}} - dk_{\text{bu}}, k_{\text{bu}}]$ the amplitude increases from $1/B_d^n N_c^3$ to 1, while the amplitude in $[k_{\text{sh}} - dk_{\text{sh}}, k_{\text{sh}}]$ is reduced from 1 to 0.

Now we examine how the energy density changes. Since we write the variations within infinitesimal phase space, it is sufficient to multiply the energy at each phase space,

$$\begin{aligned} \delta \varepsilon^{(1+2)} &= \sum_{Y=\Lambda^0, \Sigma^0} E_Y(k) \delta n_Y^{(1+2)}(k) + E_n(k) \delta n_n(k) + \delta \varepsilon_n^{\text{shell}} \\ &= \delta n_n(k) \left(-2E_Y(k) + E_n(k) + \frac{\delta \varepsilon_n^{\text{shell}}}{\delta n_n^{\text{shell}}} \right) \end{aligned} \quad (\text{C8})$$

where in the last step we used $\delta n_Y^{(1+2)}(k) = -\delta n_n(k)$ and $\delta n_n^{\text{shell}} = \delta n_n(k)$. Here $\delta \varepsilon_n^{\text{shell}}$ is

$$\delta \varepsilon_n^{\text{shell}} = -E_n(k_{\text{bu}}) \left(1 - \frac{1}{B_d^n N_c^3}\right) D(k_{\text{bu}}) dk_{\text{bu}} + E_n(k_{\text{sh}}) D(k_{\text{sh}}) dk_{\text{sh}}. \quad (\text{C9})$$

The expression $\delta \varepsilon_B^{\text{shell}} / \delta n_B^{\text{shell}}$ corresponds to the neutron chemical potential as shown in the main text. We recall that $\delta n_n(k) < 0$ corresponds to the increase of $f_Y(k)$. Looking at the coefficient of $\delta n_n(k)$, we conclude that increasing $f_Y(k)$ reduces the energy when

$$2E_Y(k) - E_n(k) \leq \frac{\delta \varepsilon_B^{\text{shell}}}{\delta n_B^{\text{shell}}}. \quad (\text{C10})$$

In the main text, we have seen that the LHS is an increasing function. Hence the inequality holds (i.e., hyperons appear) only at low momenta. Hence we conclude that the distributions f_n and f_Y take the form

$$f_n(k) = \frac{3}{2N_c^3} \Theta(k - k_Y) \Theta(k_{bu} - k) + \Theta(k - k_{bu}) \Theta(k_{sh} - k), \quad (C11)$$

$$f_Y(k) = \frac{3}{2N_c^3} \Theta(k_Y - k), \quad (C12)$$

where k_Y is defined to be

$$2E_Y(k_Y) = E_N(k_Y) + \frac{\delta \epsilon_B^{\text{shell}}}{\delta n_B^{\text{shell}}}. \quad (C13)$$

Since the distribution has the lowest energy, there should be no further conversion. Hence this condition to determine k_Y is equivalent to the β -equilibrium condition. One can manifestly compute μ_n and μ_Y using Jacobian method and check that $\mu_n = \mu_Y$ indeed holds. The results coincide with those in the main text.

-
- [1] C. Drischler, J. W. Holt, and C. Wellenhofer, Chiral Effective Field Theory and the High-Density Nuclear Equation of State, *Ann. Rev. Nucl. Part. Sci.* **71**, 403 (2021), [arXiv:2101.01709 \[nucl-th\]](#).
- [2] L. Tolos and L. Fabbietti, Strangeness in Nuclei and Neutron Stars, *Prog. Part. Nucl. Phys.* **112**, 103770 (2020), [arXiv:2002.09223 \[nucl-ex\]](#).
- [3] G. F. Burgio, H. J. Schulze, I. Vidana, and J. B. Wei, Neutron stars and the nuclear equation of state, *Prog. Part. Nucl. Phys.* **120**, 103879 (2021), [arXiv:2105.03747 \[nucl-th\]](#).
- [4] M. Baldo, G. F. Burgio, and H. J. Schulze, Hyperon stars in the Brueckner-Bethe-Goldstone theory, *Phys. Rev. C* **61**, 055801 (2000), [arXiv:nucl-th/9912066](#).
- [5] C. Drischler, S. Han, J. M. Lattimer, M. Prakash, S. Reddy, and T. Zhao, Limiting masses and radii of neutron stars and their implications, *Phys. Rev. C* **103**, 045808 (2021), [arXiv:2009.06441 \[nucl-th\]](#).
- [6] S. R. Beane, E. Chang, S. D. Cohen, W. Detmold, H. W. Lin, T. C. Luu, K. Orginos, A. Parreno, M. J. Savage, and A. Walker-Loud, Hyperon-Nucleon Interactions and the Composition of Dense Nuclear Matter from Quantum Chromodynamics, *Phys. Rev. Lett.* **109**, 172001 (2012), [arXiv:1204.3606 \[hep-lat\]](#).
- [7] T. Inoue (HAL QCD), Strange Nuclear Physics from QCD on Lattice, *AIP Conf. Proc.* **2130**, 020002 (2019), [arXiv:1809.08932 \[hep-lat\]](#).
- [8] Y. Yamamoto, H. Bando, and J. Zofka, On the Λ Hypernuclear Single Particle Energies, *Prog. Theor. Phys.* **80**, 757 (1988).
- [9] J. Guo, X.-R. Zhou, and H. J. Schulze, Skyrme force for all known Ξ - hypernuclei, *Phys. Rev. C* **104**, L061307 (2021).
- [10] A. Jinno, K. Murase, Y. Nara, and A. Ohnishi, Repulsive Λ potentials in dense neutron star matter and binding energy of Λ in hypernuclei, *Phys. Rev. C* **108**, 065803 (2023), [arXiv:2306.17452 \[nucl-th\]](#).
- [11] N. K. Glendenning and S. A. Moszkowski, Reconciliation of neutron star masses and binding of the lambda in hypernuclei, *Phys. Rev. Lett.* **67**, 2414 (1991).
- [12] J. Schaffner and I. N. Mishustin, Hyperon rich matter in neutron stars, *Phys. Rev. C* **53**, 1416 (1996), [arXiv:nucl-th/9506011](#).
- [13] S. Balberg and A. Gal, An Effective equation of state for dense matter with strangeness, *Nucl. Phys. A* **625**, 435 (1997), [arXiv:nucl-th/9704013](#).
- [14] P. Demorest, T. Pennucci, S. Ransom, M. Roberts, and J. Hessels, Shapiro Delay Measurement of A Two Solar Mass Neutron Star, *Nature* **467**, 1081 (2010), [arXiv:1010.5788 \[astro-ph.HE\]](#).
- [15] J. Antoniadis *et al.*, A Massive Pulsar in a Compact Relativistic Binary, *Science* **340**, 6131 (2013), [arXiv:1304.6875 \[astro-ph.HE\]](#).
- [16] H. T. Cromartie *et al.* (NANOGrav), Relativistic Shapiro delay measurements of an extremely massive millisecond pulsar, *Nature Astron.* **4**, 72 (2019), [arXiv:1904.06759 \[astro-ph.HE\]](#).
- [17] J. Haidenbauer, U. G. Meißner, N. Kaiser, and W. Weise, Lambda-nuclear interactions and hyperon puzzle in neutron stars, *Eur. Phys. J. A* **53**, 121 (2017), [arXiv:1612.03758 \[nucl-th\]](#).
- [18] D. Gerstung, N. Kaiser, and W. Weise, Hyperon-nucleon three-body forces and strangeness in neutron stars, *Eur. Phys. J. A* **56**, 175 (2020), [arXiv:2001.10563 \[nucl-th\]](#).
- [19] D. Lonardoni, A. Lovato, S. Gandolfi, and F. Pedivera, Hyperon Puzzle: Hints from Quantum Monte Carlo Calculations, *Phys. Rev. Lett.* **114**, 092301 (2015), [arXiv:1407.4448 \[nucl-th\]](#).
- [20] S. Weissenborn, I. Sagert, G. Pagliara, M. Hempel, and J. Schaffner-Bielich, Quark Matter In Massive Neutron Stars, *Astrophys. J. Lett.* **740**, L14 (2011), [arXiv:1102.2869 \[astro-ph.HE\]](#).
- [21] L. Bonanno and A. Sedrakian, Composition and stability of hybrid stars with hyperons and quark color-superconductivity, *Astron. Astrophys.* **539**, A16 (2012), [arXiv:1108.0559 \[astro-ph.SR\]](#).
- [22] R. Lastowiecki, D. Blaschke, H. Grigorian, and S. Typel, Strangeness in the cores of neutron stars, *Acta Phys. Polon. Supp.* **5**, 535 (2012), [arXiv:1112.6430 \[nucl-th\]](#).

- [23] T. Klöhn, R. Lastowiecki, and D. B. Blaschke, Implications of the measurement of pulsars with two solar masses for quark matter in compact stars and heavy-ion collisions: A Nambu–Jona-Lasinio model case study, *Phys. Rev. D* **88**, 085001 (2013), [arXiv:1307.6996 \[nucl-th\]](#).
- [24] K. Masuda, T. Hatsuda, and T. Takatsuka, Hadron–Quark Crossover and Massive Hybrid Stars with Strangeness, *Astrophys. J.* **764**, 12 (2013), [arXiv:1205.3621 \[nucl-th\]](#).
- [25] K. Masuda, T. Hatsuda, and T. Takatsuka, Hadron–quark crossover and massive hybrid stars, *PTEP* **2013**, 073D01 (2013), [arXiv:1212.6803 \[nucl-th\]](#).
- [26] K. Masuda, T. Hatsuda, and T. Takatsuka, Hyperon Puzzle, Hadron–Quark Crossover and Massive Neutron Stars, *Eur. Phys. J. A* **52**, 65 (2016), [arXiv:1508.04861 \[nucl-th\]](#).
- [27] T. Kojo, P. D. Powell, Y. Song, and G. Baym, Phenomenological QCD equation of state for massive neutron stars, *Phys. Rev. D* **91**, 045003 (2015), [arXiv:1412.1108 \[hep-ph\]](#).
- [28] G. Baym, T. Hatsuda, T. Kojo, P. D. Powell, Y. Song, and T. Takatsuka, From hadrons to quarks in neutron stars: a review, *Rept. Prog. Phys.* **81**, 056902 (2018), [arXiv:1707.04966 \[astro-ph.HE\]](#).
- [29] G. Baym, S. Furusawa, T. Hatsuda, T. Kojo, and H. Togashi, New Neutron Star Equation of State with Quark–Hadron Crossover, *Astrophys. J.* **885**, 42 (2019), [arXiv:1903.08963 \[astro-ph.HE\]](#).
- [30] T. Kojo, G. Baym, and T. Hatsuda, Implications of NICER for Neutron Star Matter: The QHC21 Equation of State, *Astrophys. J.* **934**, 46 (2022), [arXiv:2111.11919 \[astro-ph.HE\]](#).
- [31] J. C. Collins and M. J. Perry, Superdense Matter: Neutrons Or Asymptotically Free Quarks?, *Phys. Rev. Lett.* **34**, 1353 (1975).
- [32] L. McLerran and R. D. Pisarski, Phases of cold, dense quarks at large $N(c)$, *Nucl. Phys. A* **796**, 83 (2007), [arXiv:0706.2191 \[hep-ph\]](#).
- [33] Y. Hidaka, L. D. McLerran, and R. D. Pisarski, Baryons and the phase diagram for a large number of colors and flavors, *Nucl. Phys. A* **808**, 117 (2008), [arXiv:0803.0279 \[hep-ph\]](#).
- [34] A. Andronic *et al.*, Hadron Production in Ultra-relativistic Nuclear Collisions: Quarkyonic Matter and a Triple Point in the Phase Diagram of QCD, *Nucl. Phys. A* **837**, 65 (2010), [arXiv:0911.4806 \[hep-ph\]](#).
- [35] T. Kojo, Y. Hidaka, L. McLerran, and R. D. Pisarski, Quarkyonic Chiral Spirals, *Nucl. Phys. A* **843**, 37 (2010), [arXiv:0912.3800 \[hep-ph\]](#).
- [36] T. Kojo, Y. Hidaka, K. Fukushima, L. D. McLerran, and R. D. Pisarski, Interweaving Chiral Spirals, *Nucl. Phys. A* **875**, 94 (2012), [arXiv:1107.2124 \[hep-ph\]](#).
- [37] Y. Fujimoto, T. Kojo, and L. D. McLerran, Momentum Shell in Quarkyonic Matter from Explicit Duality: A Dual Model for Cold, Dense QCD, *Phys. Rev. Lett.* **132**, 112701 (2024), [arXiv:2306.04304 \[nucl-th\]](#).
- [38] L. McLerran and S. Reddy, Quarkyonic Matter and Neutron Stars, *Phys. Rev. Lett.* **122**, 122701 (2019), [arXiv:1811.12503 \[nucl-th\]](#).
- [39] K. S. Jeong, L. McLerran, and S. Sen, Dynamically generated momentum space shell structure of quarkyonic matter via an excluded volume model, *Phys. Rev. C* **101**, 035201 (2020), [arXiv:1908.04799 \[nucl-th\]](#).
- [40] V. Koch, L. McLerran, G. A. Miller, and V. Vovchenko, Might Normal Nuclear Matter be Quarkyonic?, (2024), [arXiv:2403.15375 \[nucl-th\]](#).
- [41] L. McLerran and G. A. Miller, The Quark Pauli Principle and the Transmutation of Nuclear Matter, (2024), [arXiv:2405.11074 \[nucl-th\]](#).
- [42] D. C. Duarte, S. Hernandez-Ortiz, and K. S. Jeong, Excluded-volume model for quarkyonic matter. II. Three-flavor shell-like distribution of baryons in phase space, *Phys. Rev. C* **102**, 065202 (2020), [arXiv:2007.08098 \[nucl-th\]](#).
- [43] D. C. Duarte, S. Hernandez-Ortiz, and K. S. Jeong, Excluded-volume model for quarkyonic Matter: Three-flavor baryon–quark Mixture, *Phys. Rev. C* **102**, 025203 (2020), [arXiv:2003.02362 \[nucl-th\]](#).
- [44] T. Zhao and J. M. Lattimer, Quarkyonic Matter Equation of State in Beta-Equilibrium, *Phys. Rev. D* **102**, 023021 (2020), [arXiv:2004.08293 \[astro-ph.HE\]](#).
- [45] J. Margueron, H. Hansen, P. Proust, and G. Chanfray, Quarkyonic stars with isospin-flavor asymmetry, *Phys. Rev. C* **104**, 055803 (2021), [arXiv:2103.10209 \[nucl-th\]](#).
- [46] T. Kojo, Stiffening of matter in quark–hadron continuity, *Phys. Rev. D* **104**, 074005 (2021), [arXiv:2106.06687 \[nucl-th\]](#).
- [47] T. Kojo and D. Suenaga, Peaks of sound velocity in two color dense QCD: Quark saturation effects and semishort range correlations, *Phys. Rev. D* **105**, 076001 (2022), [arXiv:2110.02100 \[hep-ph\]](#).
- [48] R. V. Poberezhnyuk, H. Stoecker, and V. Vovchenko, Quarkyonic matter with quantum van der Waals theory, *Phys. Rev. C* **108**, 045202 (2023), [arXiv:2307.13532 \[nucl-th\]](#).
- [49] V. Vovchenko, M. I. Gorenstein, and H. Stoecker, van der Waals Interactions in Hadron Resonance Gas: From Nuclear Matter to Lattice QCD, *Phys. Rev. Lett.* **118**, 182301 (2017), [arXiv:1609.03975 \[hep-ph\]](#).
- [50] Y. Fujimoto, K. Fukushima, Y. Hidaka, A. Hiraguchi, and K. Iida, Equation of state of neutron star matter and its warm extension with an interacting hadron resonance gas, *Phys. Lett. B* **835**, 137524 (2022), [arXiv:2109.06799 \[nucl-th\]](#).